Electronic Supplementary Material (ESI) for Journal of Materials Chemistry B.

Supporting Information

Continuous and scalable fabrication of stable and biocompatible MOF@SiO_2 nanocapsules for drug loading

*Gaofei Hu, Lili Yang, Yina Li and Leyu Wang**

State Key Laboratory of Chemical Resource Engineering, Beijing Advanced Innovation Center for Soft Matter Science and Engineering, Beijing University of Chemical Technology, Beijing 100029, China

*Email: lywang@mail.buct.edu.cn. Phone: +86-10-64433197.

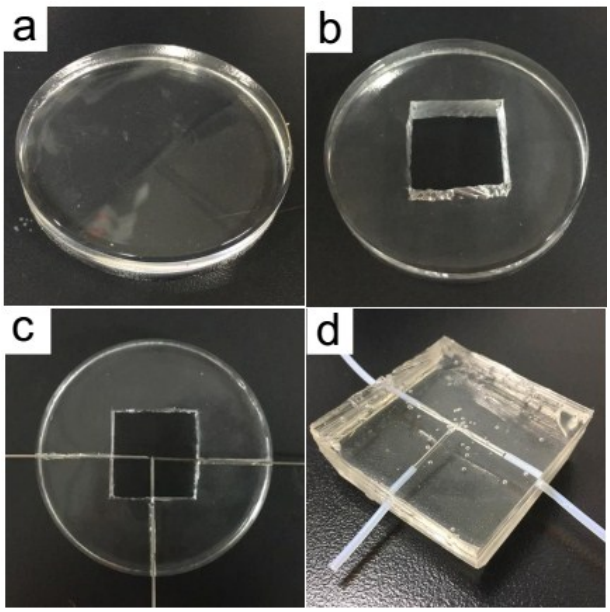

Figure S1. Illustration of the fabrication process of the PDMS template framework and the monolithic PDMS microfluidic reactor. a) PDMS precursor was poured into a petri dish and then cured to make the PDMS template; b) A square bar of PDMS was removed from the template to form a mold; c) The mold with preseted metallic needles for fabricating the microfluidic reactor; d) The microfluidic reactor was made by pouring PDMS precursor into the mold and let it solidify at 90 ℃ for 1 h.

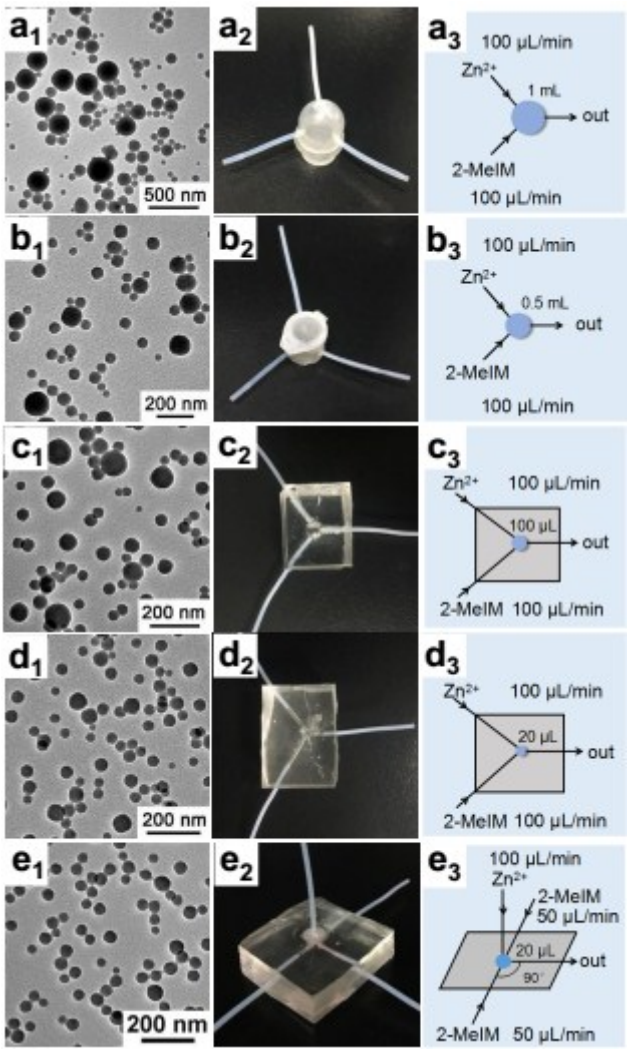

Figure S2. The evolution process of the microfluidic reactor. a1~e1) TEM images of ZIF-8 produced by the corresponding microfluidic reactors (a2~e2 photographs, and a3~e3 schematic diagrams). a~d) Optimization of the mixing volume at the junction site of the PDMS monolithic reactor, and e) 3D tubing pattern with a fixed mixing volume of 20 μL.

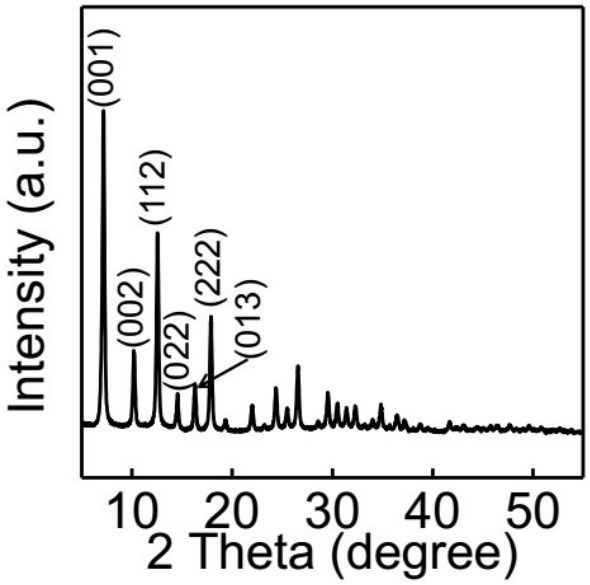

Figure S3. XRD pattern of Py@ZIF-8@SiO_2 (Py@ZS).

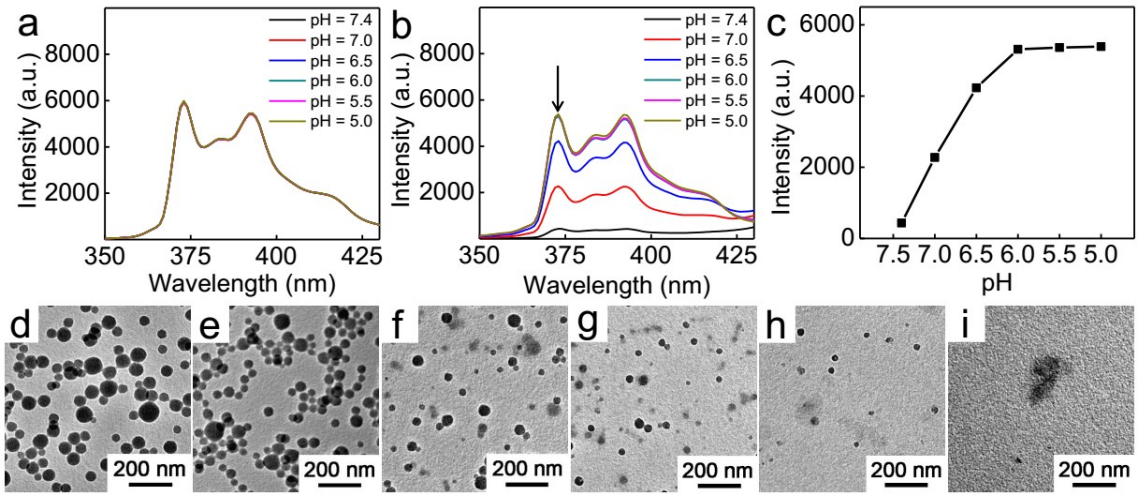

Figure S4. a) Fluorescent spectra of free pyrene (0.2 μg/mL) at different pH values (λ_{ex} = 336 nm), b) pH-responsive release of pyrene from Py@ZIF-8@SiO_2 (Py@ZS) nanocapsules, c) the evolution of luminescent intensities (at 373 nm) of pyrene released from Py@ZIF-8@SiO_2 under different pH values. d-i) TEM images of Py@ZS nanocapsules at different pH values, d) pH = 7.4, e) pH = 7.0, f) pH = 6.5, g) pH = 6.0, h) pH = 5.5, and i) pH = 5.0. As shown in the TEM images, with the decrease of pH value, the nanocapsules become smaller and smaller, and finally decompose at pH 5.0.

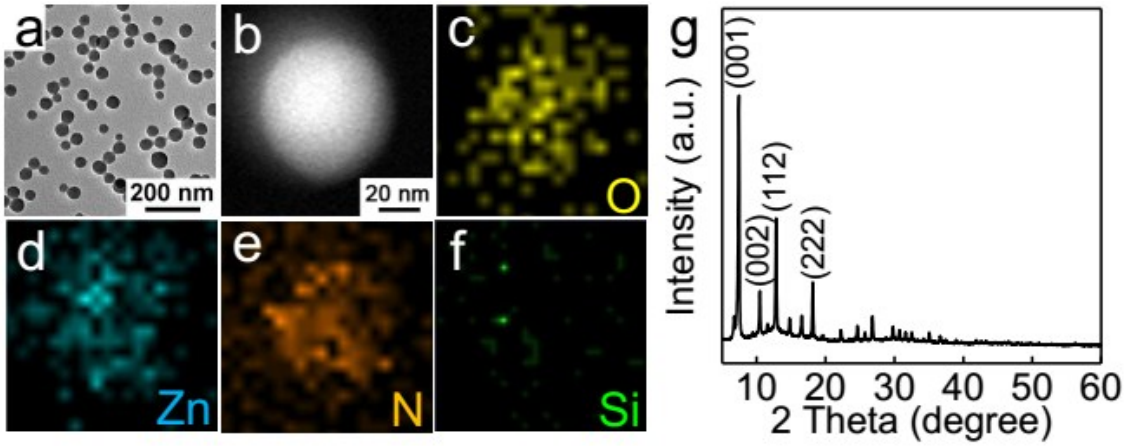

Figure S5. a) TEM image of ZIF-8; b) HAADF-STEM image of single ZIF-8 nanoparticle, and the corresponding element mapping results for c) O, d) Zn, e) N and f) Si, respectively; g) XRD pattern of ZIF-8.

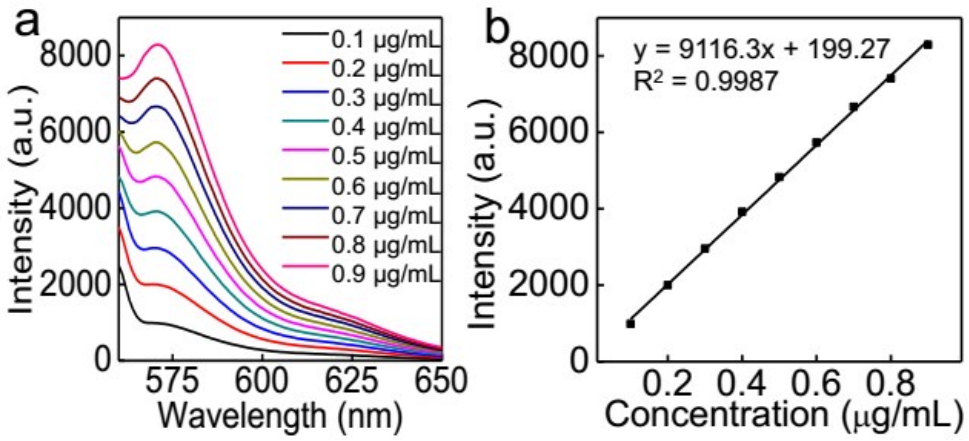

Figure S6. a) Fluorescent spectra (λ_{ex}= 532 nm) of free RB at different concentrations in PBS solution (pH 7.0), and b) the linear correlation of the fluorescent intensities (at 571 nm) versus concentrations of RB. According to the linear correlation, RB loading in RB@ZS was calculated to be 35.3 μg/mg. It is noted that RB@ZS was first decomposed in acidic solution (pH = 5.0) and then the pH was adjusted to pH 7.0 with sodium hydroxide, considering the pH dependent property of RB fluorescence.

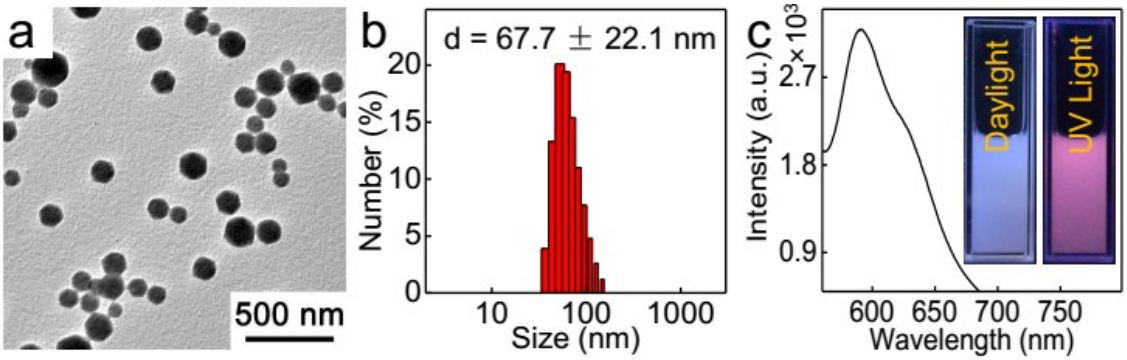

Figure S7. a) TEM image, b) DLS size distribution, and c) fluorescence spectrum (λ_{ex} = 533 nm) of DOX@ZS. Inset of c: photographs of DOX@ZS aqueous solution under daylight and UV light.

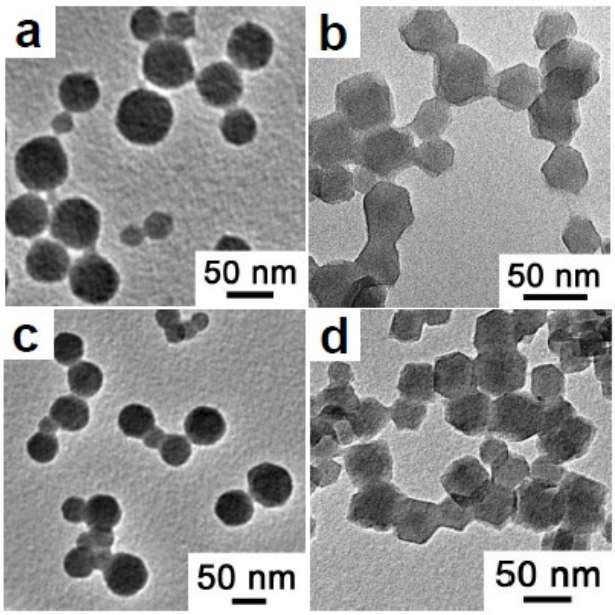

Figure S8. TEM images of ZIF-8@SiO2 (ZS) (a, b) and RB@ZS (c, d) synthesized by the microfluidic (a, c) and conventional (b, d) methods, respectively.

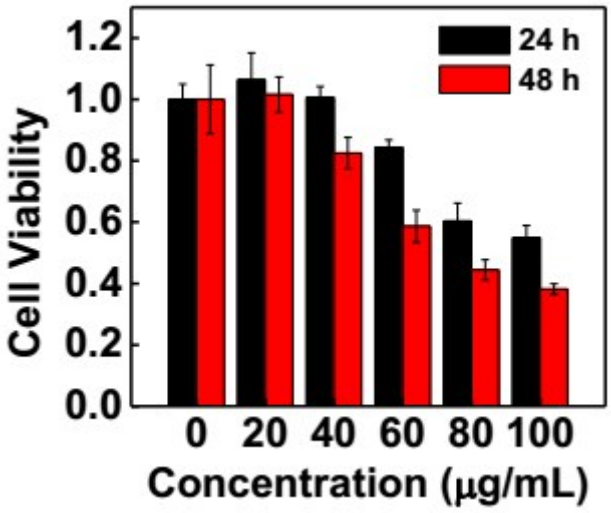

Figure S9. Cytotoxicity tests of ZIF-8 synthesized *via* the microfluidic system towards 4T1 cells for 24 h and 48 h, respectively. Four parallel measurements were conducted for each bar (n = 4).

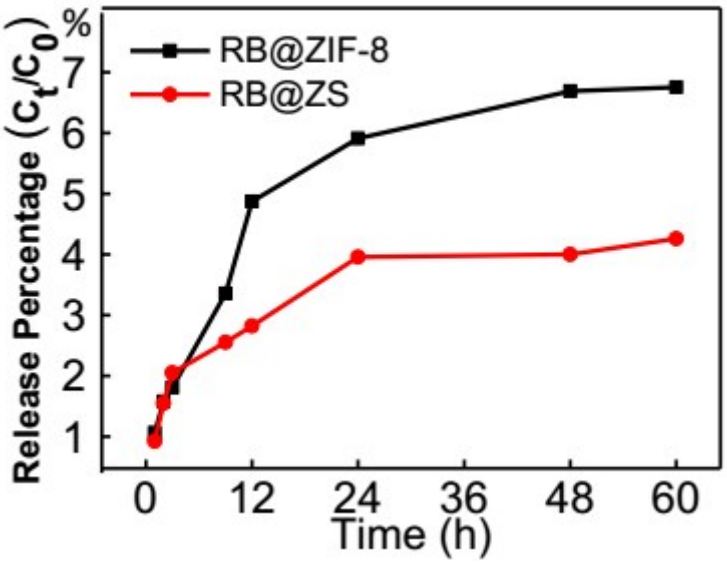

Figure S10. RB leakage from RB@ZIF-8 and RB@ZS (1.33 mg/mL) in PBS solution (pH 7.4, 10 mM) *versus* different time intervals (1, 2, 3, 9, 12, 24, 48, 60 h), respectively.

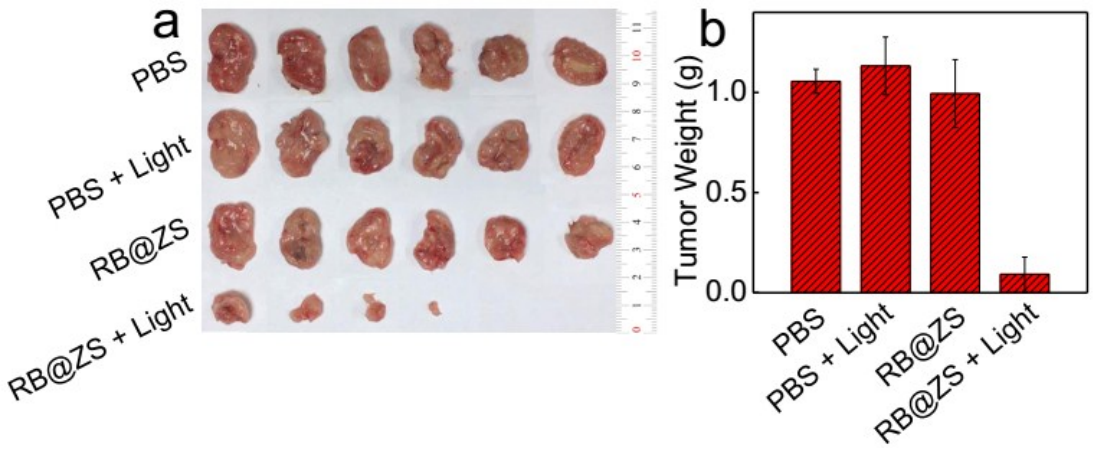

Figure S11. a) Photographs of the dissected tumors, and b) average tumor weight of different groups (n = 6) after 14 d of treatment.

Figure S12. Photographs of 4T1 tumor-bearing mice in different groups after 14 d of treatment.